

Geometric aspects of analog quantum search evolutions

Carlo Cafaro¹, Shannon Ray², and Paul M. Alsing²

¹*SUNY Polytechnic Institute, 12203 Albany, New York, USA and*

²*Air Force Research Laboratory, Information Directorate, 13441 Rome, New York, USA*

We use geometric concepts originally proposed by Anandan and Aharonov to show that the Farhi-Gutmann time optimal analog quantum search evolution between two orthogonal quantum states is characterized by unit efficiency dynamical trajectories traced on a projective Hilbert space. In particular, we prove that these optimal dynamical trajectories are the shortest geodesic paths joining the initial and the final states of the quantum evolution. In addition, we verify they describe minimum uncertainty evolutions specified by an uncertainty inequality that is tighter than the ordinary time-energy uncertainty relation. We also study the effects of deviations from the time optimality condition from our proposed Riemannian geometric perspective. Furthermore, after pointing out some physically intuitive aspects offered by our geometric approach to quantum searching, we mention some practically relevant physical insights that could emerge from the application of our geometric analysis to more realistic time-dependent quantum search evolutions. Finally, we briefly discuss possible extensions of our work to the geometric analysis of the efficiency of thermal trajectories of relevance in quantum computing tasks.

PACS numbers: Quantum computation (03.67.Lx), Quantum information (03.67.Ac), Quantum mechanics (03.65.-w).

I. INTRODUCTION

From a quantum mechanical perspective, one can modify a given state into another state by acting upon the system with a convenient Hamiltonian. In quantum computing, in particular, it is generally beneficial to know the path connecting the two states in the shortest time with the maximum speed of quantum evolution. Clearly, if the evolution occurs always at the maximum speed, one achieves time optimality by transitioning from the initial to the final state in the shortest time by taking the shortest route. Thus, the problem of connecting these quantum states can be recast in the very convenient form of a geodesic problem. From a more practical thermodynamical perspective, high speed values are not beneficial when dealing with practical devices that operate in finite time. Given the universal character of thermodynamics laws, this latter fact remains valid also for actual realizations of quantum computers. More specifically, high speeds lead to high frictional losses which, in turn, hamper the thermal efficiency of these physical systems similar to heat engines. Unfortunately, as a popular proverb says, nothing comes from free: Time optimality and thermal efficiency occur in conflicting favorable conditions. The former recommends high speeds in order to shorten the duration of the physical process. The latter, instead, welcomes low speeds to mitigate possible dissipative effects present in the system. Achieving both time optimality and thermal efficiency is a very relevant and challenging unresolved issue in quantum algorithm design [1]. Given our awareness of the importance that geometric ideas play in physics, acknowledging the power of regarding time optimality problems as geodesics problems, and given this apparently unavoidable trade-off between speed and thermal efficiency in the design of quantum algorithms, we are motivated here to study in geometric terms the efficiency of quantum evolutions of relevance in continuous-time quantum searching [2] with the hope of also providing some helpful insights into the rather complicated speed-efficiency trade-off quantification in quantum science. In what follows, we shall introduce in more detail the problem that we discuss, its motivation, and its relevance irrespective of our broader underlying interest represented by the speed-efficiency trade-off in quantum algorithms design.

In the framework of quantum search algorithms [3, 4], a geodesic path with respect to the Fubini-Study metric in the projective Hilbert space $\mathbb{C}P^{N-1}$, with $N \stackrel{\text{def}}{=} 2^n$ being the dimensionality of the complex Hilbert space \mathcal{H}_2^n of n -qubit quantum states, emerges as a curve traced by the output quantum state specifying Grover's original quantum search scheme [5–7]. In exploring for efficient quantum circuits, Riemannian geometric techniques have been exploited to reformulate the problem of finding optimal circuits into the geometric problem of finding the shortest geodesic path between two points in the curved geometry of the special unitary group $SU(N)$ [8, 9]. In the search for time-optimal quantum control protocols, differential geometry techniques have been employed to recast the quantum brachistochrone problem (for instance, see Ref. [10]) of finding a control protocol capable of taking the minimum time to achieve a desired task (for instance, the generation of a desired unitary gate) into a problem of finding a shortest geodesic path on the special unitary group $SU(N)$ [11]. Interestingly, a transition from a quantum state to an orthogonal one can be regarded as the elementary step of a computational process [12, 13]. Moreover, from an intuitive Riemannian geometric viewpoint, the optimal way of finding a solution to an arbitrary computational

problem appears to happen by “free falling” along the shortest geodesic curve connecting the (chosen) initial and (desired) final states on the appropriate curved manifold that characterizes the specific problem being analyzed [8].

The work that we present in this article takes into account three key ideas: i) The reformulation of a time-optimal problem into a geodesic problem [11]; ii) The consideration that the most elementary step of a computational process can be described in terms of a quantum mechanical transition between two orthogonal states [12, 13]; iii) The intuition that optimal solutions of computational tasks can be geometrically described in terms of shortest geodesic paths [8]. In particular, we are motivated here by the following questions: Can we geometrically characterize the efficiency of quantum search schemes? Can we geometrically quantify the effect of experimentally tunable parameters on the performance of quantum search algorithms? Can we generate some fresh physical insight leading to a (currently non-existing) geometric measure of thermal efficiency given the fact that good quantum algorithms need to be both fast and thermodynamically efficient? More specifically, we wish to enhance in this article our understanding of the time optimality of the original Farhi-Gutmann quantum search Hamiltonian evolution [2] between the generally nonorthogonal source and target states by gaining new insights with the use of Riemannian geometric tools as originally proposed by Anandan and Aharonov in Ref. [14]. In their work, Anandan and Aharonov introduced the efficiency of a quantum evolution as $\eta \stackrel{\text{def}}{=} s_0/s$ with s_0 being the length of the geodesic path connecting the initial and final quantum states of the system, while s denotes the length of the path generated by the actual Hamiltonian evolution. To our knowledge, there are currently no explicit applications of η in the literature, which obscures both its physical meaning and its potential practical usefulness.

In this article, we present the first application of the geometric efficiency of quantum evolutions using the Farhi-Gutmann quantum search Hamiltonian [2] as an example. Given our previously mentioned considerations in i), ii), and iii), we want to study the geometry of this quantum search evolution between two orthogonal quantum states. In particular, we wish to determine whether or not to a time optimal quantum search scheme, whose analysis is based upon the concept of transition probability, there corresponds a maximally efficient quantum search evolution achieving the ideal unit efficiency value. Such a determination will be made in the scenario wherein the output quantum state originating from the quantum search scheme traces a shortest geodesic path connecting the suitably chosen initial and final orthogonal states on the projective space (that is, the Bloch sphere $\mathbb{C}P^1$ in the case of single-qubit quantum states) equipped with the Fubini-Study metric. Furthermore, we wish to understand how deviations (see Ref. [15]) from optimal quantum search schemes can be described within the proposed Riemannian geometric framework and discuss any physical insight that may arise from this theoretical description. Finally, we wish to determine whether or not there exists any possibility of extending this geometric characterization of quantum evolutions to the Riemannian geometric study of thermal trajectories [16–18]. The pursuit of such an extension is undertaken with the hope of proposing a good geometric measure of thermal efficiency for thermodynamical processes of interest in quantum information science [1] by improving upon our recent results in Refs. [19, 20].

The layout of the remainder of this article is as follows. In Section II, we briefly present the essential features of both the original and the modified Farhi-Gutmann quantum search Hamiltonians. In particular, for each scheme, we highlight both transition probabilities from the source to the target states and the minimum search times yielding the maximum success probabilities. In Section III, we introduce the essential features of the geometric structure of quantum evolutions. More specifically, we describe the concept of a geodesic line on the Bloch sphere and explain how to quantify a departure from a geodesic evolution. In Section IV, we discuss a geometric measure of efficiency for a quantum evolution together with its connection with a form of time-energy uncertainty inequality to be satisfied during the physical evolution at all times. In Section V, we study the geodesicity, the efficiency, and the uncertainty inequality for both the original and modified Farhi-Gutmann quantum search algorithms. We present our concluding remarks in Section VI. Finally, some technical details can be found in Appendix A and Appendix B.

II. QUANTUM SEARCH HAMILTONIANS

In this Section, we briefly discuss the main properties of both the original [2] and the modified [2, 15] Farhi-Gutmann quantum search algorithms. In particular, for each scheme, we emphasize both transition probabilities from the source to the target states and the minimum search times leading to the maximum success probabilities.

A. The original scenario

Quantum search algorithms, including Grover’s original quantum search scheme [3], were originally proposed in a digital quantum computation framework in terms of a discrete sequence of unitary logic gates. By contrast, Farhi and Gutmann used an analog quantum computation setting to present an analog version of Grover’s original quantum search algorithm in which the state of the quantum register undergoes a continuous time evolution under the action of

a conveniently selected driving Hamiltonian [2]. The essential idea of the continuous time search algorithm proposed by Farhi and Gutmann can be summarized as follows. Given an Hamiltonian acting on an N -dimensional (with $N \stackrel{\text{def}}{=} 2^n$) complex vector space \mathcal{H}_2^n with a single nonvanishing eigenvalue $E \neq 0$ and all others being zero, find the eigenvector $|w\rangle$ that has eigenvalue equal to E . The search is completed when the quantum system is known to be in the state $|w\rangle$. Working with time-independent Hamiltonian evolutions, Farhi and Gutmann proved that their algorithm required a minimum search time of the order \sqrt{N} , thus being characterized by the same complexity as Grover's original quantum search algorithm. The full original Farhi-Gutmann quantum search Hamiltonian is given by [2],

$$\mathbf{H}_{\text{FG}} \stackrel{\text{def}}{=} \mathbf{H}_w + \mathbf{H}_d = E |w\rangle \langle w| + E |s\rangle \langle s|, \quad (1)$$

with $\mathbf{H}_w \stackrel{\text{def}}{=} E |w\rangle \langle w|$ and $\mathbf{H}_d \stackrel{\text{def}}{=} E |s\rangle \langle s|$ being the oracle and driving Hamiltonians, respectively. The normalized states $|s\rangle$ and $|w\rangle$ are the source (initial) and target (final) states, respectively. The target state $|w\rangle$ is a randomly chosen (unknown) state from the unit sphere in \mathcal{H}_2^n , while the source state $|s\rangle$ is some suitably selected normalized vector that does not depend on $|w\rangle$. The source state $|s\rangle$ evolves according to Schrödinger's quantum mechanical evolution law [21],

$$|s\rangle \mapsto |\psi(t)\rangle \stackrel{\text{def}}{=} e^{-\frac{i}{\hbar} \mathbf{H}_{\text{FG}} t} |s\rangle. \quad (2)$$

Moreover, without loss of generality, the quantum overlap $x \stackrel{\text{def}}{=} \langle w|s\rangle \neq 0$ can be taken to be real and positive because any phase factor in the inner product between these two states can be eventually incorporated in $|s\rangle$. Moreover, given that it is sufficient to focus our attention to the two-dimensional subspace of \mathcal{H}_2^n spanned by $|s\rangle$ and $|w\rangle$, it is convenient to introduce the orthonormal basis $\{|w\rangle, |r\rangle\}$ with $|r\rangle \stackrel{\text{def}}{=} (1-x^2)^{-1/2} (|s\rangle - x|w\rangle)$ and $|s\rangle \stackrel{\text{def}}{=} x|w\rangle + \sqrt{1-x^2}|r\rangle$, respectively. Working with the basis $\{|w\rangle, |r\rangle\}$, it is possible to show that the probability $\mathcal{P}_{\text{FG}}(t)$ of finding the state $|w\rangle$ at time time t is given by [2],

$$\mathcal{P}_{\text{FG}}(t) \stackrel{\text{def}}{=} \left| \langle w|e^{-\frac{i}{\hbar} \mathbf{H}_{\text{FG}} t}|s\rangle \right|^2 = \sin^2 \left(\frac{Ex}{\hbar} t \right) + x^2 \cos^2 \left(\frac{Ex}{\hbar} t \right). \quad (3)$$

In particular, the (smallest) instant t_{FG} at which the transition probability $\mathcal{P}_{\text{FG}}(t)$ assumes its maximum value $\mathcal{P}_{\text{FG}}^{\text{max}} = 1$ is,

$$t_{\text{FG}} \stackrel{\text{def}}{=} \frac{\pi \hbar}{2Ex}. \quad (4)$$

When the target state $|w\rangle$ is assumed to be an element of a set of mutually orthonormal quantum states $\{|a\rangle\}$ with $1 \leq a \leq N$ of \mathcal{H}_2^n , the source state $|s\rangle$ can be conveniently chosen as an equal superposition of the N quantum states $\{|a\rangle\}$. Then, $x = 1/\sqrt{N}$ and from Eq. (4) we note that $t_{\text{FG}} \propto \sqrt{N}$. Thus, in analogy to Grover's search, the Farhi-Gutmann algorithm requires a minimum search time of the order \sqrt{N} . Additionally, by assuming that the target state is an unknown element of a given orthonormal basis $\{|a\rangle\}$ with $1 \leq a \leq N$ of \mathcal{H}_2^n that is produced with absolute certainty, Farhi and Gutmann proved that their algorithm is optimally short.

B. The modified scenario

Before considering their optimality proof, Farhi and Gutmann pointed out in Ref. [2] that one may be driven by intuition to believe that by using a different driving Hamiltonian $\mathbf{H}'_d \stackrel{\text{def}}{=} E' |s\rangle \langle s|$ with $E' \gg E$, one could shorten the search time by speeding up the procedure for finding the target state $|w\rangle$. More explicitly, consider the full modified Farhi-Gutmann quantum search Hamiltonian given by [2, 15],

$$\mathbf{H}_{\text{MFG}} \stackrel{\text{def}}{=} \mathbf{H}_w + \mathbf{H}'_d = E |w\rangle \langle w| + E' |s\rangle \langle s|, \quad (5)$$

where $\mathbf{H}_w \stackrel{\text{def}}{=} E |w\rangle \langle w|$ and $\mathbf{H}'_d \stackrel{\text{def}}{=} E' |s\rangle \langle s|$ with $E' \gg E$. Following the analysis performed in the original scenario, it can be shown that the probability $\mathcal{P}_{\text{MFG}}(t)$ of finding the state $|w\rangle$ at time time t is given by [15],

$$\mathcal{P}_{\text{MFG}}(t) \stackrel{\text{def}}{=} \frac{x^2 (E' + E)^2}{4x^2 E' E + (E' - E)^2} \sin^2 \left(\frac{1}{2\hbar} \sqrt{4x^2 E E' + (E' - E)^2} t \right) + x^2 \cos^2 \left(\frac{1}{2\hbar} \sqrt{4x^2 E E' + (E' - E)^2} t \right). \quad (6)$$

Observe that for $E = E'$, we recover from Eq. (6) the expression of $\mathcal{P}_{\text{FG}}(t)$ in Eq. (3). Moreover, the (smallest) instant t_{MFG} at which the transition probability $\mathcal{P}_{\text{MFG}}(t)$ assumes its maximum value $\mathcal{P}_{\text{MFG}}^{\text{max}} = \left[x^2 (E' + E)^2 \right] / \left[4x^2 E' E + (E' - E)^2 \right] < 1$ is,

$$t_{\text{MFG}} \stackrel{\text{def}}{=} \frac{\pi \hbar}{\sqrt{4x^2 E' E + (E' - E)^2}}. \quad (7)$$

As expected, when $E' = E$, t_{MFG} in Eq. (7) reduces to t_{FG} in Eq. (4). Clearly, by comparing the transition probabilities in Eqs. (3) and (6), we are able to conclude in a transparent manner that using a modified driving Hamiltonian $H'_d \stackrel{\text{def}}{=} E' |s\rangle \langle s|$ with $E' \gg E$ does not speed up the procedure for producing the target state $|w\rangle$ with certainty. Indeed, although t_{MFG} in Eq. (7) is smaller than t_{FG} in Eq. (4), we note that $\mathcal{P}_{\text{MFG}}^{\text{max}} < \mathcal{P}_{\text{FG}}^{\text{max}} = 1$. Therefore, while the Hamiltonian H_{MFG} may have some merit in nearly optimal quantum search schemes as pointed out in Ref. [15], it appears to be less “efficient” than H_{FG} and consequently, does not lead to any advantage in the context of quantum search with certainty as one may have thought from a classically intuitive point of view. Despite the Farhi-Gutmann formal optimality proof and the Cafaro-Alsing brute force transition probability analysis, it remains interesting to consider whether or not the different “efficiency” of the quantum search schemes specified by the Hamiltonians H_{FG} and H_{MFG} can be understood in neat geometric terms that might be closer to our intuition. Motivated by this main thought, we propose in what follows a geometric perspective on the efficiency of these two analog quantum search schemes.

III. GEODESICS IN RAY SPACE

In this Section, we introduce basic geometric concepts of quantum evolutions with emphasis on the unitary Schrödinger evolution.

Let \mathcal{H}_2^n denote an $N \stackrel{\text{def}}{=} 2^n$ -dimensional complex Hilbert space of n -qubit (normalized) quantum states $\{|\psi\rangle\}$. Since the global phase of a vector state is not observable, a physical state is represented by a so-called ray of the Hilbert space. The set of rays of \mathcal{H}_2^n is called the (complex) projective Hilbert space $\mathbb{C}P^{N-1}$. Formally speaking, $\mathbb{C}P^{N-1}$ is the quotient set of \mathcal{H}_2^n by the equivalence relation $|\psi\rangle \sim e^{i\beta} |\psi\rangle$ with $\beta \in \mathbb{R}$. The space $\mathbb{C}P^{N-1}$ can be equipped with a mathematically correct and physically meaningful metric structure. Indeed, consider a family $\{|\psi(\xi)\rangle\}$ of normalized quantum states of \mathcal{H}_2^n that smoothly depend on an m -dimensional parameter $\xi \stackrel{\text{def}}{=} (\xi^1, \dots, \xi^m) \in \mathbb{R}^m$. Then, the ordinary Hermitian scalar product on \mathcal{H}_2^n induces a metric tensor $g_{ab}(\xi)$ with $1 \leq a, b \leq m$ on the manifold of quantum states defined as [22],

$$g_{ab}(\xi) \stackrel{\text{def}}{=} 4 \text{Re} [\langle \partial_a \psi(\xi) | \partial_b \psi(\xi) \rangle - \langle \partial_a \psi(\xi) | \psi(\xi) \rangle \langle \psi(\xi) | \partial_b \psi(\xi) \rangle], \quad (8)$$

with $\partial_a \stackrel{\text{def}}{=} \partial / \partial \xi^a$. The quantity $g_{ab}(\xi)$ in Eq. (8) is the so-called Fubini-Study metric tensor. In particular, we note that the metric is positive definite as is evident by considering the distance element ds_{FS}^2 between two nearby points with associated vector states $|\psi(\xi + d\xi)\rangle$ and $|\psi(\xi)\rangle$ [23],

$$ds_{\text{FS}}^2 \stackrel{\text{def}}{=} g_{ab}(\xi) d\xi^a d\xi^b = 4 \left[\langle d\psi | d\psi \rangle - |\langle \psi | d\psi \rangle|^2 \right], \quad (9)$$

where $|d\psi\rangle \stackrel{\text{def}}{=} |\psi(\xi + d\xi)\rangle - |\psi(\xi)\rangle$. The distance element in Eq. (9) leads naturally to the concept of geodesic paths in $\mathbb{C}P^{N-1}$. Indeed, by using variational calculus arguments, geodesic paths in $\mathbb{C}P^{N-1}$ can be obtained by minimizing the distance integral S [24],

$$S \stackrel{\text{def}}{=} \int ds_{\text{FS}} = 2 \int \left[\langle d\psi | d\psi \rangle - |\langle \psi | d\psi \rangle|^2 \right]^{1/2} = \int \mathcal{L} d\tau, \quad (10)$$

with $\mathcal{L} \stackrel{\text{def}}{=} 2 \left[\langle \dot{\psi} | \dot{\psi} \rangle - \left| \langle \dot{\psi} | \psi \rangle \right|^2 \right]^{1/2}$, $|\dot{\psi}\rangle \stackrel{\text{def}}{=} \partial_\tau |\psi\rangle$, and τ being a parameter along the curve $\gamma(\tau) : \tau \mapsto |\psi(\tau)\rangle$ that we assume to be equal to the natural parameter $s_{\text{FS}} = s$. We recall that if $|\psi(s)\rangle$ is a geodesic then the phase-transformed vector $|\bar{\psi}(s)\rangle \stackrel{\text{def}}{=} e^{i\beta(s)} |\psi(s)\rangle$ with arbitrary $\beta(s)$ is also a geodesic [24]. In particular, by conveniently choosing $\beta(s)$ such that $\langle \bar{\psi}(s) | \bar{\psi}'(s) \rangle = 0$ with $|\bar{\psi}'(s)\rangle \stackrel{\text{def}}{=} \partial_s |\bar{\psi}(s)\rangle$ (that is, $|\bar{\psi}(s)\rangle$ is the horizontal lift of $|\psi(s)\rangle$

satisfying the parallel transport rule), it can be shown after some straightforward but tedious variational calculus computations that a geodesic $|\bar{\psi}(s)\rangle$ satisfies a simple harmonic oscillator equation [25, 26],

$$|\bar{\psi}''(s)\rangle + |\bar{\psi}(s)\rangle = 0. \quad (11)$$

Assuming $\langle \bar{\psi}(0) | \bar{\psi}(0) \rangle = 1$, $\langle \bar{\psi}(0) | \bar{\psi}'(0) \rangle = 0$, and $\langle \bar{\psi}'(0) | \bar{\psi}'(0) \rangle = \omega^2$ with ω being a constant in \mathbb{R} , the solution of Eq. (11) can be written as,

$$|\bar{\psi}(s)\rangle = \cos(\omega s) |\bar{\psi}(0)\rangle + \frac{\sin(\omega s)}{\omega} |\bar{\psi}'(0)\rangle. \quad (12)$$

Eq. (12) represents the most general geodesic in horizontal and affinely parameterized form in CP^{N-1} [25]. More generally, it can be shown that any two arbitrary unit vectors $|\psi_A\rangle$ and $|\psi_B\rangle$ in the projective Hilbert space can be connected by a geodesic line $|\psi_{\text{geo}}(\lambda)\rangle$ parametrized by a real parameter $0 \leq \lambda \leq 1$ [25, 27],

$$|\psi_{\text{geo}}(\lambda)\rangle \stackrel{\text{def}}{=} \frac{(1-\lambda)|\psi_A\rangle + e^{i\phi}\lambda|\psi_B\rangle}{\sqrt{1-2\lambda(1-\lambda)[1-|\langle\psi_B|\psi_A\rangle|]}}, \quad (13)$$

where $|\psi_{\text{geo}}(0)\rangle = |\psi_A\rangle$, $|\psi_{\text{geo}}(1)\rangle = |\psi_B\rangle$, and $\phi \in \mathbb{R}$ with $\langle\psi_B|\psi_A\rangle = |\langle\psi_B|\psi_A\rangle|e^{i\phi}$. For the sake of completeness, we emphasize that a simple explicit way to check that $|\psi_{\text{geo}}(\lambda)\rangle$ does indeed represent a geodesic line is to show that the length of the curve connecting $|\psi_A\rangle$ and $|\psi_B\rangle$ measured with the Fubini-Study metric equals the minimal possible length of the curve on the Bloch sphere connecting these two states. Upon recasting Eq. (13) as,

$$|\psi_{\text{geo}}(\theta)\rangle \stackrel{\text{def}}{=} \frac{\cos(\frac{\theta}{2})|\psi_A\rangle + e^{i\phi}\sin(\frac{\theta}{2})|\psi_B\rangle}{\sqrt{1+\sin(\theta)|\langle\psi_B|\psi_A\rangle|}}, \quad (14)$$

with $\lambda = \lambda(\theta) \stackrel{\text{def}}{=} \tan(\theta/2) / [1 + \tan(\theta/2)]$ being a strictly monotonic function of θ where $0 \leq \theta \leq \pi$, it can be shown that the length $s \stackrel{\text{def}}{=} \int_0^\pi \sqrt{ds_{\text{FS}}^2}$ of this curve equals $2\cos^{-1}[|\langle\psi_B|\psi_A\rangle|]$. This, in turn, coincides with the Wootters distance or, equivalently, the angle between the two states $|\psi_A\rangle$ and $|\psi_B\rangle$ [28]. Thus, $|\psi_{\text{geo}}(\lambda)\rangle$ and $|\psi_{\text{geo}}(\theta)\rangle$ in Eqs. (13) and (14) respectively, are indeed geodesic arcs. We point out that in Eqs. (13) and (14), it is assumed that $|\psi_A\rangle$ and $|\psi_B\rangle$ are nonorthogonal. When $|\psi_A\rangle \perp |\psi_B\rangle$, geodesic lines can be obtained from Eqs. (13) and (14) by taking $\phi = 0$ and, clearly, $\langle\psi_B|\psi_A\rangle = 0$. One way to determine whether or not Schrödinger's solution $|\psi(t)\rangle$ specifies a geodesic path is to verify that the geodesic curvature of its corresponding dynamical trajectory on the Bloch sphere is identically zero. Alternatively, a more convenient approach available to us is to check whether there exists a reversible mapping $\lambda : (0, t_*) \ni t \mapsto \lambda(t) \in (0, 1)$ with $\lambda(0) = 0$ and $\lambda(t_*) = 1$ such that the distance $d^2(t, \lambda)$ between $|\psi(t)\rangle$ and $|\psi_{\text{geo}}(\lambda)\rangle$ in Eq. (14),

$$d^2(t, \lambda) \stackrel{\text{def}}{=} 4 \left[1 - |\langle\psi(t) | \psi_{\text{geo}}(\lambda)\rangle|^2 \right], \quad (15)$$

is identically zero. As a final remark of geometric flavor, we point out that horizontal affinely parametrized geodesics on the Bloch sphere are great circles traced by state vectors as in Eq. (12) [22, 29, 30].

The quantum material presented in Section II together with the geometric material covered in Section III will be helpful in putting the concepts of efficiency and uncertainty of search evolutions to be introduced in the next Section in the proper geometric formulation of quantum evolutions as originally proposed by Anandan and Aharonov in Ref. [14].

IV. EFFICIENCY AND UNCERTAINTY OF QUANTUM EVOLUTIONS

In this Section, following the work by Anandan and Aharonov in Ref. [14], we discuss a geometric measure of efficiency for a quantum search evolution together with its connection to a form of time-energy uncertainty inequality, with the latter being fulfilled at all times during the physical evolution of the system under consideration.

A. Efficiency

Consider a quantum mechanical evolution of a state vector $|\psi(t)\rangle$ described by the Schrödinger equation,

$$i\hbar\partial_t |\psi(t)\rangle = H(t) |\psi(t)\rangle, \quad (16)$$

with $0 \leq t \leq t_*$. Following the work by Anandan and Aharonov, a geometric measure of efficiency for such a quantum evolution can be formally defined as [14],

$$\eta \stackrel{\text{def}}{=} 1 - \frac{\Delta s}{s} = \frac{2 \cos^{-1} [|\langle \psi(0) | \psi(t_*) \rangle|]}{2 \int_0^{t_*} \frac{\Delta E(t')}{\hbar} dt'}, \quad (17)$$

where $\Delta s \stackrel{\text{def}}{=} s - s_0$, s_0 denotes the distance along the shortest geodesic path joining the distinct initial $|\psi(0)\rangle$ and final $|\psi(t_*)\rangle$ states on the projective Hilbert space $\mathbb{C}P^{N-1}$ and finally, s is the distance along the actual dynamical trajectory traced by the state vector $|\psi(t)\rangle$ with $0 \leq t \leq t_*$. Observe that the numerator in Eq. (17) is the angle between the state vectors $|\psi(0)\rangle$ and $|\psi(t_*)\rangle$ and equals the Wootters distance ds_{Wootters} [28],

$$ds_{\text{Wootters}}(|\psi(t_1)\rangle, |\psi(t_2)\rangle) \stackrel{\text{def}}{=} 2 \cos^{-1} [|\langle \psi(t_1) | \psi(t_2) \rangle|]. \quad (18)$$

The denominator in Eq. (17) instead, is the integral of the infinitesimal distance ds along the evolution curve (that is, the actual dynamical trajectory) in the projective Hilbert space [14],

$$ds \stackrel{\text{def}}{=} 2 \frac{\Delta E(t)}{\hbar} dt, \quad (19)$$

with ΔE being the square root of the dispersion (or equivalently, the variance) of the Hamiltonian operator $H(t)$,

$$\Delta E(t) \stackrel{\text{def}}{=} \left[\langle \psi | H^2(t) | \psi \rangle - \langle \psi | H(t) | \psi \rangle^2 \right]^{1/2}. \quad (20)$$

Interestingly, Anandan and Aharonov showed that the infinitesimal distance ds in Eq. (19) is related to the Fubini-Study infinitesimal distance $ds_{\text{Fubini-Study}}$ by the following relation,

$$ds_{\text{Fubini-Study}}^2(|\psi(t)\rangle, |\psi(t+dt)\rangle) \stackrel{\text{def}}{=} 4 \left[1 - |\langle \psi(t) | \psi(t+dt) \rangle|^2 \right] = 4 \frac{\Delta E^2(t)}{\hbar^2} dt^2 + \mathcal{O}(dt^3), \quad (21)$$

with $\mathcal{O}(dt^3)$ denoting an infinitesimal quantity equal or higher than dt^3 . From Eqs. (19) and (21), it follows that s is proportional to the time integral of the uncertainty in energy ΔE of the system and represents the distance along the quantum evolution of the physical system in $\mathbb{C}P^{N-1}$ as measured by the Fubini-Study metric. We point out that when the actual dynamical curve coincides with the shortest geodesic path connecting the initial and final states, Δs equals zero and the efficiency η in Eq. (17) becomes one. Clearly, the shortest possible distance between two orthogonal quantum states on $\mathbb{C}P^{N-1}$ is π while, in general $s \geq \pi$ for such a pair of orthogonal pure states. These considerations will become especially useful in Section V. For the interested readers, we confine a brief discussion on possible generalizations of η in Eq. (17) to geometric evolutions of mixed quantum states not limited to temporal unitary propagators in Appendix A. In the next subsection, we elaborate on the concept of uncertainty of a quantum search evolution.

B. Uncertainty

In quantum theory [21], the standard quantum mechanical uncertainty relation given by

$$\Delta x \Delta p \geq \hbar/2, \quad (22)$$

reflects the intrinsic randomness of the outcomes of quantum experiments. Specifically, if one repeats many times the same state preparation scheme and then measures the operators x or p , the variety of observations recorded for x and p are characterized by standard deviations Δx and Δp whose product $\Delta x \Delta p$ is greater than $\hbar/2$. In particular, Gaussian wave packets (for instance, the ground state of a shifted harmonic oscillator) are specified by a minimum position-momentum uncertainty with $\Delta x \Delta p = \hbar/2$.

In the geometry of quantum evolutions, there exists an analog of Eq. (22) on the one hand, while on the other, Gaussian wave packets are replaced by geodesic paths in the projective Hilbert space. Indeed, consider the time-averaged uncertainty in energy $\langle \Delta E \rangle$ during a time interval Δt_{\perp} defined as [14],

$$\langle \Delta E \rangle \stackrel{\text{def}}{=} \frac{1}{\Delta t_{\perp}} \int_0^{\Delta t_{\perp}} E(t') dt'. \quad (23)$$

The quantity Δt_{\perp} in Eq. (23) represents the orthogonalization time, that is, the time interval during which the system passes from an initial state $|\psi_A\rangle \stackrel{\text{def}}{=} |\psi(0)\rangle$ to a final state $|\psi_B\rangle \stackrel{\text{def}}{=} |\psi(\Delta t_{\perp})\rangle$ where $\langle\psi_B|\psi_A\rangle = \delta_{AB}$. Using Eqs. (19) and (23) and recalling that the shortest possible distance between two orthogonal quantum states on $\mathbb{C}P^{N-1}$ is π , we get

$$\Delta \stackrel{\text{def}}{=} \langle\Delta E\rangle \Delta t_{\perp} \geq h/4. \quad (24)$$

In particular, it is only when the quantum evolution is a geodesic evolution that the equality in Eq. (24) holds. Thus, just as Gaussian wave packets are minimum position-momentum uncertainty wave packets, geodesic paths are minimum time-averaged energy uncertainty trajectories. In summary, unit efficiency $\eta = 1$ is achieved when a quantum evolution has minimum uncertainty $\langle\Delta E\rangle \Delta t_{\perp} = h/4$. This, in turn, happens only if the physical systems moves along a geodesic path in $\mathbb{C}P^{N-1}$. Interestingly, the Anandan-Aharonov time-energy uncertainty relation in Eq. (24) can be linked to the statistical speed of evolution ds_{FS}/dt of the physical system with ds_{FS}^2 being the Fubini-Study infinitesimal line element squared. Specifically, since $ds_{\text{FS}}/dt = \Delta E(t)/\hbar$, the physical system moves expeditiously wherever the uncertainty in energy is large.

The concept of geodesic line mentioned in Section III together with the concepts of efficiency and uncertainty presented in this Section will be used in the next Section in order to geometrically analyze the quantum search evolutions described in Section II.

V. GEODESICITY, EFFICIENCY, AND UNCERTAINTY OF QUANTUM SEARCH EVOLUTIONS

In this Section, we aim to study the geodesicity condition $d^2(t, \lambda) = 0$ with $d^2(t, \lambda)$ in Eq. (15), the efficiency in Eq. (17), and the uncertainty inequality in Eq. (24) for both the original and modified Farhi-Gutmann quantum search algorithms presented in Section II.

A. The original scenario

Considering the original Farhi-Gutmann scenario, the state vector $|\psi(t)\rangle$ that solves the Schrödinger evolution relation in Eq. (16) with $H = H_{\text{FG}}$ in Eq. (1) such that $|\psi_A\rangle = |\psi(0)\rangle$, $|\psi_B\rangle = |\psi(t_*)\rangle$, $\langle\psi_B|\psi_A\rangle \xrightarrow{x \rightarrow 0} \delta_{AB}$ with $x \stackrel{\text{def}}{=} \langle w|s\rangle$, and $t_* = \Delta t_{\perp} = t_{\text{FG}}$ with t_{FG} defined in Eq. (4) is given by,

$$|\psi(t)\rangle = \frac{1}{\sqrt{2}} \frac{e^{-\frac{i}{\hbar}Et}}{\sqrt{1 - \sqrt{1 - x^2}}} \left((1 - \sqrt{1 - x^2}) \cos\left(\frac{Ex}{\hbar}t\right) - ix \sin\left(\frac{Ex}{\hbar}t\right) \right). \quad (25)$$

Substituting Eqs. (13) and (25) into $d^2(t, \lambda)$ in Eq. (15), we obtain

$$d_{\text{FG}}^2(t, \lambda) = 4 \left\{ 1 - \left[\frac{(1 - \lambda)^2 \cos^2\left(\frac{Ex}{\hbar}t\right)}{1 - 2\lambda(1 - \lambda)} + \frac{\lambda^2 \sin^2\left(\frac{Ex}{\hbar}t\right)}{1 - 2\lambda(1 - \lambda)} + \frac{\lambda(1 - \lambda) \sin\left(\frac{2Ex}{\hbar}t\right) \cos\left(\frac{\pi}{2x}\right)}{1 - 2\lambda(1 - \lambda)} \right] \right\}. \quad (26)$$

Finally, we impose $d^2(t, \lambda)$ equal to zero so as to find possible roots $\{\lambda(t)\}$. Then, in order to obtain a well-defined reversible mapping $\lambda : (0, t_*) \ni t \mapsto \lambda(t) \in (0, 1)$ with $\lambda(0) = 0$ and $\lambda(t_*) = 1$, we find it is necessary to have $t_* = t_{\text{FG}}(x) \stackrel{\text{def}}{=} \pi\hbar/(2Ex)$ with $x \in (0, 1)$ such that

$$\frac{\pi}{2x} = 2n\pi, \quad (27)$$

with $n \in \mathbb{N}$. Finally, given that Eq. (27) is clearly solvable, we find that a suitable reversible mapping $\lambda(t)$ is given by

$$\lambda(t) \stackrel{\text{def}}{=} \frac{\sin^2\left(\frac{E}{4\hbar}t\right) + \frac{1}{2} \sin\left(\frac{E}{2\hbar}t\right)}{1 + \sin\left(\frac{E}{2\hbar}t\right)}. \quad (28)$$

Indeed, it is straightforward to check that $d_{\text{FG}}^2(t, \lambda) = 0$ by substituting Eqs. (27) and (28) into Eq. (26). Interestingly, observe that $\lambda(t)$ in Eq. (28) is a strictly monotonic increasing function of t with $0 \leq t \leq t_*$ and is such that $\lambda(t_*/2) = 1/2$. We remark that we have shown that the Farhi-Gutmann Hamiltonian evolution trajectory between

the two orthogonal quantum states $|\psi_A\rangle$ and $|\psi_B\rangle$ is formally a geodesic in the limiting scenario in which the quantum overlap x approaches zero, that is, the duration of the evolution t_{FG} approaches infinity (long-time-limit). This limit requires formally selecting a very large value of n in Eq. (27) when defining our reversible mapping $\lambda = \lambda(t)$. This requirement is physically consistent with the fact that t_{FG} , being inversely proportional to x , tends to diverge when the Farhi-Gutmann Hamiltonian evolution occurs between nearly orthogonal source and target quantum states. It is in this regime that we conduct our analysis of Farhi-Gutmann and modified Farhi-Gutmann trajectories in this paper. For additional comments on this point, we refer to Appendix B. Finally, by substituting Eq. (25) into the efficiency η given in Eq. (17) and the time-energy uncertainty inequality presented in Eq. (24), we obtain

$$\eta_{\text{FG}} = 1, \text{ and } \Delta_{\text{FG}} \stackrel{\text{def}}{=} [(\Delta E) \Delta t_{\perp}]_{\text{FG}} = h/4, \quad (29)$$

respectively. Thus by investigating the geometry of the original Farhi-Gutmann quantum evolution, we are able to conclude that it describes a geodesic motion on the Bloch sphere specified by unit efficiency η_{FG} and a minimum uncertainty Δ_{FG} that reaches the minimum achievable value of $h/4$.

B. The modified scenario

Within the context of the modified Farhi-Gutmann scenario, the state vector $|\psi(t)\rangle$ that solves the Schrödinger evolution relation in Eq. (16) with $H = H_{\text{MFG}}$ in Eq. (5) such that $|\psi_A\rangle = |\psi(0)\rangle$, $|\psi_B\rangle = |\psi(t_*)\rangle$, $\langle\psi_B|\psi_A\rangle \xrightarrow{x \rightarrow 0} \delta_{AB}$ with $x \stackrel{\text{def}}{=} \langle w|s\rangle$, and $t_* = \Delta t_{\perp} = t_{\text{MFG}}$ with t_{MFG} defined in Eq. (7) is given by,

$$|\psi(t)\rangle = e^{-\frac{i}{\hbar} \frac{E'+E}{2} t} \begin{pmatrix} \cos\left(\frac{\lambda}{\hbar} t\right) + i \frac{A+B}{A-B} \sin\left(\frac{\lambda}{\hbar} t\right) & -2i \frac{AB}{A-B} \sin\left(\frac{\lambda}{\hbar} t\right) \\ \frac{2i}{A-B} \sin\left(\frac{\lambda}{\hbar} t\right) & \cos\left(\frac{\lambda}{\hbar} t\right) - i \frac{A+B}{A-B} \sin\left(\frac{\lambda}{\hbar} t\right) \end{pmatrix} |\psi(0)\rangle. \quad (30)$$

The initial state $|\psi(0)\rangle$ in Eq. (30) is defined as,

$$|\psi(0)\rangle \stackrel{\text{def}}{=} \begin{pmatrix} \frac{\sqrt{(1-AB)^2 + (A+B)^2} - (1-AB)}{\sqrt{(A+B)^2 + (\sqrt{(1-AB)^2 + (A+B)^2} - (1-AB))^2}} \\ \frac{A+B}{\sqrt{(A+B)^2 + (\sqrt{(1-AB)^2 + (A+B)^2} - (1-AB))^2}} \end{pmatrix}, \quad (31)$$

where the quantities $A = A(x, E', E)$ and $B = B(x, E', E)$ are explicitly given by

$$A(x, E', E) \stackrel{\text{def}}{=} \frac{1}{2xE'\sqrt{1-x^2}} \left[E - E' + 2x^2 E' - \sqrt{4x^2 E E' + (E' - E)^2} \right], \quad (32)$$

and,

$$B(x, E', E) \stackrel{\text{def}}{=} \frac{1}{2xE'\sqrt{1-x^2}} \left[E - E' + 2x^2 E' + \sqrt{4x^2 E E' + (E' - E)^2} \right], \quad (33)$$

respectively. Finally, the quantity $\lambda = \lambda(x, E', E)$ in Eq. (30) is defined as

$$\lambda(x, E', E) \stackrel{\text{def}}{=} \frac{1}{2} \sqrt{4x^2 E E' + (E' - E)^2}. \quad (34)$$

We recall that the states in Eqs. (25) and (30) are expressed in terms of the orthonormal basis $\{|w\rangle, |r\rangle\}$ introduced in Section II. Substituting Eqs. (13) and (30) into $d^2(t, \lambda)$ in Eq. (15), leads to

$$\frac{d_{\text{MFG}}^2(t, \lambda)}{4} = \left\{ 1 - \left[\frac{(1-\lambda)^2 \cos^2\left(\frac{\lambda}{\hbar} t\right)}{1-2\lambda(1-\lambda)} + \frac{\lambda^2 \sin^2\left(\frac{\lambda}{\hbar} t\right)}{1-2\lambda(1-\lambda)} + \frac{\lambda(1-\lambda) \sin\left(\frac{2\lambda}{\hbar} t\right) \cos\left(\frac{\pi}{2} \frac{E'+E}{\sqrt{4x^2 E E' + (E' - E)^2}}\right)}{1-2\lambda(1-\lambda)} \right] \right\}. \quad (35)$$

Finally, proceeding as before, we impose $d^2(t, \lambda)$ equal to zero so as to find possible roots $\{\lambda(t)\}$. Then, in order to obtain a well-defined reversible mapping $\lambda : (0, t_*) \ni t \mapsto \lambda(t) \in (0, 1)$ with $\lambda(0) = 0$ and $\lambda(t_*) = 1$, we observe that it is necessary to have $t_* = t_{\text{MFG}}(x) \stackrel{\text{def}}{=} \pi \hbar / (\sqrt{4x^2 E E' + (E' - E)^2})$ with $x \in (0, 1)$ such that

$$\frac{\pi}{2} \frac{E' + E}{\sqrt{4x^2 E E' + (E' - E)^2}} = 2n\pi, \quad (36)$$

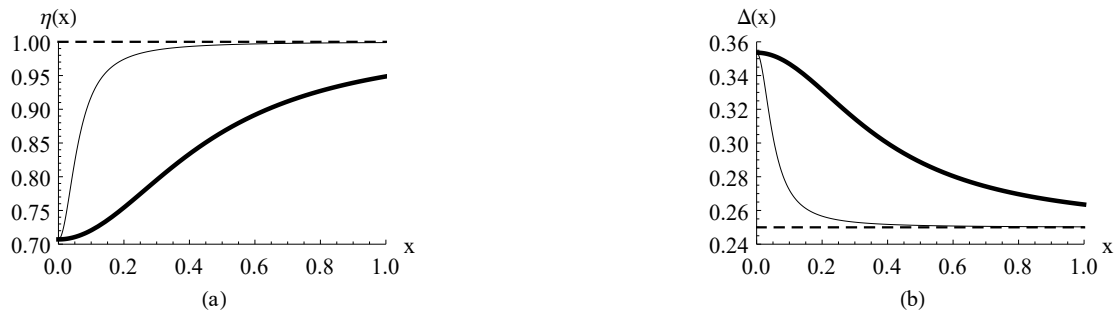


FIG. 1: Part (a): Efficiency η versus the quantum overlap x in the case of $\gamma = 1$ (dashed line), $\gamma = 1.1$ (thin solid line), and $\gamma = 2$ (thick solid line). Part (b): Uncertainty Δ versus the quantum overlap x in the case of $\gamma = 1$ (dashed line), $\gamma = 1.1$ (thin solid line), and $\gamma = 2$ (thick solid line). The original and modified Farhi-Gutmann scenarios are specified by $\gamma \stackrel{\text{def}}{=} E'/E = 1$ and $\gamma > 1$, respectively.

with arbitrary $n \in \mathbb{N}$. Unlike Eq. (27) however, there does not exist any real value $x \in (0, 1)$ in the modified physical scenario of interest with $E' \gg E$ (that is, $\gamma \gg 1$ with $E' \stackrel{\text{def}}{=} \gamma E$) presented in Section II and originally proposed by Farhi and Gutmann. Indeed, assuming such a working condition, Eq. (36) yields $x^2 \stackrel{E' \gg E}{\approx} [(1 - 16n^2)/64n^2] (E'/E)$. Thus, Eq. (36) has no solutions for x belonging to the interval of interest that yields $d^2(t, \lambda)$ identically equal to zero. For a discussion on the small energy difference regime, we refer to Appendix B. In summary, given the impossibility of finding a well-defined reversible mapping between the geodesic line in Eq. (13) and the dynamical trajectory traced by the state vector in Eq. (30), we conclude that the modified Farhi-Gutmann quantum evolution is not described by a geodesic path on the Bloch sphere.

Finally, by substituting Eq. (30) into the efficiency η given in Eq. (17) and the time-energy uncertainty inequality presented in Eq. (24), we obtain

$$\eta_{\text{MFG}}(x, E', E) = \frac{1}{\sqrt{2}} \left[\frac{(E' - E)^2 + 4x^2 E' E}{(E' - E)^2 + 2x^2 E' E} \right]^{1/2} < 1 \quad (37)$$

and,

$$\Delta_{\text{MFG}}(x, E', E) \stackrel{\text{def}}{=} [\langle \Delta E \rangle \Delta t_{\perp}]_{\text{MFG}} = \frac{h}{2\sqrt{2}} \left[\frac{(E' - E)^2 + 2x^2 E' E}{(E' - E)^2 + 4x^2 E' E} \right]^{1/2} > h/4, \quad (38)$$

respectively, for any $E' > E$. Thus, by studying the geometry of the modified Farhi-Gutmann quantum evolution, we arrive at the conclusion that it does not describe a geodesic motion on the Bloch sphere, is specified by a non-maximal efficiency $\eta_{\text{MFG}}(x, E', E)$ and the minimum uncertainty $\Delta_{\text{MFG}}(x, E', E)$ is greater than the minimum achievable value of $h/4$. For the sake of simplicity, we set the Planck constant h equal to one. Finally, for the sake of clarity, we plot the efficiency η and the uncertainty Δ as a function of the quantum overlap $x \in (0, 1)$ for a number of fixed values of the ratio $\gamma \stackrel{\text{def}}{=} E'/E \geq 1$ in Fig. 1.

VI. CONCLUDING REMARKS

In this article, we employed Riemannian geometric concepts to show that time optimal analog quantum search evolutions between two orthogonal quantum states are characterized by unit efficiency (see Eq. (29)) dynamical trajectories traced on a projective Hilbert space. In particular, we proved that these optimal dynamical trajectories are the shortest geodesic paths joining the initial and the final states of the quantum evolution (see Eqs. (26), (27), and (28)). In addition, we verified that they describe minimum uncertainty evolutions specified by an uncertainty inequality that is tighter than the ordinary time-energy uncertainty relation (see Eq. (29)). Furthermore, we studied the effects of deviations from the time optimality condition from our proposed Riemannian geometric perspective. In particular, by geometric means we found that deviations from the original Farhi-Gutmann Hamiltonian evolution lead

Quantum Evolution	Motion on Bloch Sphere	Uncertainty of Evolution	Efficiency of Evolution
original Farhi-Gutmann	geodesic	$\Delta = h/4$, minimal	$\eta = 1$, maximal
modified Farhi-Gutmann	non-geodesic	$\Delta > h/4$, non-minimal	$\eta < 1$, non-maximal

TABLE I: Illustrative representation of the type of motion on the Bloch sphere, uncertainty of evolution, and efficiency of evolution corresponding to both the original and the modified Farhi-Gutmann quantum search Hamiltonian evolutions.

to non-geodesic motion on the Bloch sphere (see Eqs. (35) and (36)), to non-maximal efficiency (see Eq. (37)) and, finally, to non-minimal uncertainty of the evolution (see Eq. (38)). A summary of our main results can be visualized in Fig. 1 and are reported in Table I.

We believe that despite its simplicity, the relevance of our work is threefold. Firstly, our Riemannian geometric analysis of quantum search evolutions offers an alternate theoretical perspective on the concept of optimality with intuitive physical insights arising from familiar concepts such as shortest path, maximal efficiency, and minimal uncertainty. In this respect, it becomes especially relevant when taken into consideration together with Refs. [2, 15]. Secondly, it could potentially help providing a practical and systematic way of constructing efficient search schemes. Indeed, this construction could occur by ranking the maximal achievable efficiencies of the various search schemes while tuning parameters of physical relevance that specify the more realistic time-dependent Hamiltonian at hand [31, 32]. For instance, it would be of interest to extend the simple analysis presented here to time-dependent quantum search Hamiltonians yielding either on-resonance or off-resonance scenarios [20, 33]. In such a case, the set of experimentally tunable parameters would include, for instance, the energy gap between two quantum states, the frequency of the external drive field, and the strength of the external drive field as discussed in Ref. [32]. Thirdly, given that realistic quantum algorithms are expected to be both fast and thermodynamically efficient [1], our work can be regarded as a model to emulate in order to find a good geometric measure of efficiency for thermodynamic processes. Our preliminary results along these lines have recently appeared in Refs. [19, 20]. Roughly speaking, the main idea is to replace the geometry of quantum evolutions with the geometry of thermodynamic processes [16, 17], Schrodinger's quantum trajectories with thermal trajectories [18] and, finally, shortest paths on the Bloch sphere with coolest paths on the manifold of thermal states [34–36]. Clearly, one may wonder how to introduce a notion of thermodynamical efficiency in this quantum searching context. We remark that in the modified scenario with $E' \gg E$, the system moves along a non-geodesic path connecting the initial and final orthogonal states with a speed $v_{\text{MGF}} = (2/\hbar)\Delta E_{\text{MFG}} > \pi/\Delta t_{\perp}^{(\text{MFG})}$. However, despite exhibiting a speed higher than the one that would specify an evolution of geodesic type, the modified scenario is not energetically favorable since the minimal Anandan-Aharonov minimum time-energy uncertainty condition is violated (that is, $\Delta_{\text{MFG}} > h/4$) with the consequence that the efficiency as defined in Eq. (17) of this particular quantum mechanical evolution is suboptimal. These considerations, emerging from this specific physical scenario considered within the framework of quantum search Hamiltonian evolutions, are reminiscent of the speed-efficiency trade-off mentioned in our Introduction. At this stage, however, we can only speculate on the issue of defining a good measure of thermodynamic efficiency in the context of quantum searching. To be more specific, our next set of explorative steps in this direction includes the following points: i) a better understanding of the analogies between quantum mechanical and thermodynamical relations [18, 37]; ii) a deeper comprehension of the methods of thermodynamic geometry employed to identify optimal driving protocols that minimize the dissipative losses of the underlying thermal processes [36]; iii) an extensive understanding of the geometry of evolutions of open quantum systems with particular emphasis on the determination of time-optimal evolutions of impure quantum states [37]; iv) a quantitative understanding of the possible beneficial effects of dissipation in quantum searching with the inclusion of thermodynamical arguments [38]. We believe, for instance, that one of the relevant outcomes of this cross fertilization between geometry, quantum, and thermal physics will be a more systematic hybrid method of identifying constructive use of dissipation in quantum searching. In particular, we expect that the identification tool will be a measure of efficiency to get to the target state from a given initial state that is geometrically characterized by a suitable cost function that ideally maximizes quantum speed and minimizes thermal dissipation at the same time. Of course, these are mere conjectures at this point and we shall keep pursuing these fascinating avenues of investigations in our future scientific efforts.

Acknowledgments

C.C. is grateful to the United States Air Force Research Laboratory (AFRL) Summer Faculty Fellowship Program for providing support for this work. S.R. acknowledges support from the National Research Council Research Associate Fellowship program (NRC-RAP). P.M.A. acknowledges support from the Air Force Office of Scientific Research (AFOSR). Any opinions, findings and conclusions or recommendations expressed in this material are those of the

author(s) and do not necessarily reflect the views of the Air Force Research Laboratory (AFRL).

-
- [1] D. Castelvecchi, *Clash of the physics laws*, Nature (London) **543**, 597 (2017).
- [2] E. Farhi and S. Gutmann, *Analog analogue of a digital quantum computation*, Phys. Rev. **A57**, 2403 (1998).
- [3] L. K. Grover, *Quantum mechanics helps in searching for a needle in a haystack*, Phys. Rev. Lett. **79**, 325 (1997).
- [4] M. A. Nielsen and I. L. Chuang, *Quantum Computation and Quantum Information*, Cambridge University Press (2000).
- [5] J. J. Alvarez and C. Gomez, *A comment on Fisher information and quantum algorithms*, arXiv:quant-ph/9910115 (2000).
- [6] A. Miyake and M. Wadati, *Geometric strategy for the optimal quantum search*, Phys. Rev. **A64**, 042317 (2001).
- [7] C. Cafaro, *Geometric algebra and information geometry for quantum computational software*, Physica **A470**, 154 (2017).
- [8] M. A. Nielsen, M. R. Dowling, M. Gu, and A. C. Doherty, *Quantum computation as geometry*, Science **311**, 1133 (2006).
- [9] H. E. Brandt, *Riemannian curvature in the differential geometry of quantum computation*, Physica **E42**, 449 (2010).
- [10] A. Carlini, A. Hosoya, T. Koike, and Y. Okudaira, *Time-optimal quantum evolution*, Phys. Rev. Lett. **96**, 060503 (2006).
- [11] X. Wang, M. Allegra, K. Jacobs, S. Lloyd, C. Lupo, and M. Mohseni, *Quantum brachistochrone as geodesics: Obtaining accurate control protocols for time-optimal quantum gates*, Phys. Rev. Lett. **114**, 170501 (2015).
- [12] L. B. Levitin, *Physical limitations of rate, depth, and minimum energy in information processing*, Int. J. Theor. Phys. **21**, 299 (1982).
- [13] L. B. Levitin and T. Toffoli, *Fundamental limit on the rate of quantum dynamics: The unified bound is tight*, Phys. Rev. Lett. **103**, 160502 (2009).
- [14] J. Anandan and Y. Aharonov, *Geometry of quantum evolution*, Phys. Rev. Lett. **65**, 1697 (1990).
- [15] C. Cafaro and P. M. Alsing, *Theoretical analysis of a nearly optimal analog quantum search*, Physica Scripta **94**, 085103 (2019).
- [16] G. Ruppeiner, *Riemannian geometry in thermodynamic fluctuation theory*, Rev. Mod. Phys. **67**, 605 (1995).
- [17] H. Quevedo, *Geometrothermodynamics*, J. Math. Phys. **48**, 013506 (2007).
- [18] D. C. Brody and L. P. Hughston, *Geometry of thermodynamic states*, Phys. Lett. **A245**, 73 (1998).
- [19] C. Cafaro and P. M. Alsing, *Decrease of Fisher information and the information geometry of evolution equations for quantum mechanical probability amplitudes*, Phys. Rev. **E97**, 042110 (2018).
- [20] C. Cafaro and P. M. Alsing, *Information geometry aspects of minimum entropy production paths from quantum mechanical evolutions*, Phys. Rev. **E101**, 022110 (2020).
- [21] A. Peres, *Quantum Theory: Concepts and Methods*, Kluwer Academic Publishers (1995).
- [22] J. P. Provost and G. Vallee, *Riemannian structure on manifolds of quantum states*, Commun. Math. Phys. **76**, 289 (1980).
- [23] S. Braunstein and C. M. Caves, *Statistical distance and the geometry of quantum states*, Phys. Rev. Lett. **72**, 3439 (1994).
- [24] A. N. Grigorenko, *Geometry of projective Hilbert space*, Phys. Rev. **A46**, 7292 (1992).
- [25] N. Mukunda and R. Simon, *Quantum kinematic approach to the geometric phase.I. General formalism*, Annals of Physics **228**, 205 (1993).
- [26] A. K. Pati, *On phases and length of curves in a cyclic quantum evolution*, Pramana-J. Phys. **42**, 455 (1994).
- [27] H. P. Laba and V. M. Tkachuk, *Geometric characteristics of quantum evolution: Curvature and torsion*, Condensed Matter Physics **20**, 1 (2017).
- [28] W. K. Wootters, *Statistical distance and Hilbert space*, Phys. Rev. **D23**, 357 (1981).
- [29] J. Samuel and R. Bhandari, *General setting for Berry's phase*, Phys. Rev. Lett. **60**, 2339 (1988).
- [30] I. Bengtsson and K. Życzkowski, *Geometry of Quantum States*, Cambridge University Press (2006).
- [31] C. Cafaro and P. M. Alsing, *Continuous-time quantum search and time-dependent two-level quantum systems*, Int. J. Quantum Information **17**, 1950025 (2019).
- [32] F. Wilczek, H.-Y. Hu, and B. Wu, *Resonant quantum search with monitor qubits*, Chinese Phys. Lett. **37**, 050304 (2020).
- [33] C. Cafaro, S. Gassner, and P. M. Alsing, *Information geometric perspective on off-resonance effects in driven two-level quantum systems*, Quantum Reports **2**, 166 (2020).
- [34] L. Diosi, K. Kulacsy, B. Lukacs, and A. Racz, *Thermodynamic length, time, speed, and optimum path to minimize entropy production*, J. Chem. Phys. **105**, 11220 (1996).
- [35] M. Scandi and M. Perarnau-Llobet, *Thermodynamic length in open quantum systems*, Quantum **3**, 197 (2019).
- [36] K. Brandner and K. Saito, *Thermodynamic geometry of microscopic heat engines*, Phys. Rev. Lett. **124**, 040602 (2020).
- [37] E. Sjöqvist, *Geometry along evolution of mixed quantum states*, Phys. Rev. Research **2**, 013344 (2020).
- [38] A. Mizel, *Critically damped quantum search*, Phys. Rev. Lett. **102**, 150501 (2009).
- [39] M.M. Wilde, *Quantum Information*, Cambridge University Press (2017).
- [40] M. M. Taddei, B. M. Escher, L. Davidovich, and R. L. de Matos Filho, *Quantum speed limits for physical processes*, Phys. Rev. Lett. **110**, 050402 (2013).
- [41] N. Horeh and A. Mann, *Intelligent states for the Anandan-Aharonov parameter-based uncertainty relation*, J. Phys. **A: Math. Gen.** **31**, L609 (1998).
- [42] S. Boixo, S. T. Flammia, C. M. Caves, and JM Geremia, *Generalized limits for single-parameter quantum estimation*, Phys. Rev. Lett. **98**, 090401 (2007).
- [43] S. L. Braunstein, C. M. Caves, and G. J. Milburn, *Generalized uncertainty relations: Theory, examples, and Lorentz invariance*, Annals of Physics **247**, 135 (1996).

- [44] V. Giovannetti, S. Lloyd, and L. Maccone, *Quantum metrology*, Phys. Rev. Lett. **96**, 010401 (2006).
- [45] R. J. Birrittella, P. M. Alsing, and C. C. Gerry, *The parity operator: Applications in quantum metrology*, under review in AVS Quantum Science: Special Topic: Quantum Sensing and Metrology (August, 2020); arXiv:quant-ph/2008.08658.
- [46] S. Gassner, C. Cafaro, and S. Capozziello, *Transition probabilities in generalized quantum search Hamiltonian evolutions*, Int. Journal of Geometric Methods in Modern Physics **17**, 2050006 (2020).

Appendix A: Geometric efficiency beyond pure states and time-propagators

In this Appendix, we emphasize several technical details concerning the manner in which our measure of efficiency η in Eq. (17) can be readily extended to more general physical processes.

Our expression for the efficiency Eq. (17) can be written and interpreted in several forms as shown below

$$\eta \stackrel{\text{def}}{=} \frac{s_0}{s} = \frac{\int_{\text{geo}} ds_{\text{Wootters}}}{\int_{\text{H}} ds_{\text{FS}}} = \frac{2 \cos^{-1} [|\langle \psi(0) | \psi(t_*) \rangle|]}{2 \int_0^{t_*} \frac{\Delta E(t')}{\hbar} dt'} = \frac{2 \theta_B}{2 \int_0^{t_*} \frac{\Delta E(t')}{\hbar} dt'}. \quad (\text{A1})$$

The first equality in Eq. (A1) defines the efficiency η as the ratio of two lengths, which by the second equality shows is the ratio of the Wootters distance along the geodesic connecting the initial and final states $|\psi(0)\rangle$ and $|\psi(t_*)\rangle$ to the integrated Fubini-Study distance along the path generated by the Hamiltonian H . This later ratio is given by the third equality. As interpreted in the main text, the last inequality uses the fact that for pure states, the numerator defines the Bures angle θ_B [30] via $\cos(\theta_B) = \sqrt{F}$ where for pure states $\sqrt{F} = |\langle \psi(0) | \psi(t_*) \rangle|$ is the Uhlmann Fidelity between the initial and final state $|\psi(0)\rangle$ and $|\psi(t_*)\rangle$. The Bures angle is related to the Bures distance d_B [30] via $d_B^2 = 2(1 - \sqrt{F}) = 4 \sin^2(\theta_B/2)$, so that we could have also written the numerator of Eq. (A1) in terms of this length as $2\theta_B = 4 \sin^{-1}(d_B/2)$. For infinitesimally close states this gives $\theta_B \approx d_B$. Thus, we see that our efficiency considered as a ratio of geometric lengths is intimately related to the quantum mechanical concept of the fidelity between the initial and final states.

The concept of fidelity is generalized from pure to mixed states via the Uhlmann-Jozsa [30, 39] fidelity $F[\rho(0), \rho(t_*)] \stackrel{\text{def}}{=} \left[\text{tr} \left(\sqrt{\rho(0)\rho(t_*)\rho(0)} \right) \right]^2$ which arises from the overlap of the pure state $|\psi_\rho(0)\rangle$ and $|\psi_\rho(t_*)\rangle$ *purifications* of the initial and final states $\rho(0)$ and $\rho(t_*)$, maximized over an arbitrary unitary in the higher dimensional purification Hilbert space. (Note that: $\text{tr}_R[|\psi_\rho\rangle\langle\psi_\rho|] = \rho$, where the purified state $|\psi_\rho\rangle$ lives in the composite Hilbert space $\mathcal{H}_R \otimes \mathcal{H}_S$ of system- S (ρ) and reservoir- R). The Bures angle and Bures distance retain their pure-state form [30], i.e. $\cos(\theta_B) = \sqrt{F}[\rho(0), \rho(t_*)]$ and $d_B^2 = 2(1 - \sqrt{F}[\rho(0), \rho(t_*)])$. Note that the fidelity is a *total* distance in the sense that its computation only relies upon the knowledge of the state at either end of the geodesic that connects the initial and final state. One might ask if there is some differential quantity for which the fidelity is the integrated version along the geodesic. The answer is yes, and this quantity is the Quantum Fisher Information (QFI). This leads to a new interpretation of the denominator in Eq. (A1).

Let us note that $\mathcal{F}_Q(t) \stackrel{\text{def}}{=} \text{tr}[\rho(t)L^2(t)]$ denotes the quantum Fisher information for time estimation along the trajectory specified by the system evolution, and $L(t)$ is the so-called symmetric logarithmic derivative operator defined in an implicit fashion by the equation $d\rho/dt = [\rho(t)L(t) + L(t)\rho(t)]/2$ [23]. Moreover, the connection between $\mathcal{F}_Q(t)$ in the denominator of η in Eq. (A1) and the dispersion $\Delta E(t)$ of the Hamiltonian operator H in the denominator of η in Eq. (17) can be made transparent by observing that the analogue of $|\langle \psi(t) | \psi(t+dt) \rangle|^2 = 1 - [\Delta E^2(t)/\hbar^2] dt^2 + O(dt^3)$ is $F(t, t+dt) = 1 - [\mathcal{F}_Q(t)/4] dt^2 + O(dt^3)$ for mixed quantum states [40]. Therefore, the square root $\sqrt{\mathcal{F}_Q(t)}$ of the quantum Fisher information replaces $2[\Delta E(t)/\hbar]$ for pure states and is generally proportional to the instantaneous speed of separation between two infinitesimally closed mixed quantum states. This allows us to write the efficiency in terms of the fidelities as

$$\eta \stackrel{\text{def}}{=} \frac{s_0}{s} = \frac{2 \cos^{-1} \left(\sqrt{F}[\rho(0), \rho(t_*)] \right)}{\int_0^{t_*} \sqrt{\mathcal{F}_Q(t')} dt'}, \quad (\text{A2})$$

which now holds in general for mixed states.

Secondly, the Hamiltonian operator H and the temporal parameter t can be replaced by any other Hermitian operator A_ξ (for instance, the number operator, the momentum operator, or the angular momentum along the quantization axis) and any arbitrary parameter ξ (for instance, the phase of a clock or the strength of an external field), respectively.

The parameter ξ describes the evolution of the physical system by the action of the unitary operator $U_{A_\xi}(\xi) \stackrel{\text{def}}{=} e^{\frac{i}{\hbar} \xi A_\xi}$ which replaces the usual Schrödinger time-propagator. As a consequence, the usual Anandan-Aharonov time-energy uncertainty inequality, $\langle \Delta E \rangle \Delta t_\perp \geq \hbar/4$, can be generalized to assume the form $\Delta A_\xi \delta \xi \geq \hbar/4$ with $\delta \xi$ being essentially the precision with which ξ can be determined [41]. In addition, we remark that for pure states the quantum Fisher information is a multiple of the variance of A_ξ . For mixed states, instead, the variance provides only an upper bound on the Fisher information [42]. Therefore, given this intimate connection between the quantum Fisher information and the variance of the Hermitian generator A_ξ of the displacements in ξ , the usual Anandan-Aharonov time-energy uncertainty inequality can be regarded as being replaced by a generalized uncertainty relation, $\delta \xi \geq (\hbar/2) \mathcal{F}_\xi^{-1/2}(t)$, that derives from the Cramer-Rao bound that appears in precision quantum metrology [43–45].

Lastly, it should be noted that along the geodesic, i.e. the shortest distance connecting the initial and final states, we have $\int_{0, \text{geo}}^{t^*} \sqrt{\mathcal{F}_Q(t')} dt' = \sqrt{F}[\rho(0), \rho(t_*)]$ so that the QFI is the infinitesimal version of the quantum fidelity. Further, along any longer (non-geodesic) path ($s > s_0$) generated by a Hamiltonian H , we have $\int_{0, H}^{t^*} \sqrt{\mathcal{F}_Q(t')} dt' \leq \sqrt{F}[\rho(0), \rho(t_*)]$. This allows us to generalize the concept of efficiency $0 \leq \eta \rightarrow \tilde{\eta} \leq 1$ to a quantity involving the only ratio of fidelities and/or of integrated QFIs along the optimal geodesic (s_0) and the evolved (under H) path ($s > s_0$)

$$\eta = \frac{s_0}{s} \longleftrightarrow \tilde{\eta} \stackrel{\text{def}}{=} \frac{\int_{0, H}^{t^*} \sqrt{\mathcal{F}_Q(t')} dt'}{\sqrt{F}[\rho(0), \rho(t_*)]_{\text{geo}}} = \frac{\int_{0, H}^{t^*} \sqrt{\mathcal{F}_Q(t')} dt'}{\int_{0, \text{geo}}^{t^*} \sqrt{\mathcal{F}_Q(t')} dt'}. \quad (\text{A3})$$

Both measures of efficiencies η and $\tilde{\eta}$ quantify the same concepts, in terms of inverse ratios, relating the initial and final states of the system: (i) the geometric point of view: $\eta = s_0/s \leq 1$, i.e. the length along the path generated by H is *greater* than the optimal (shortest) geodesic path, and (ii) the fidelity/QFI point of view: $\tilde{\eta} \leq 1$, i.e. the fidelity, or integrated QFI, along the path generated by H is *less* than that of along the optimal path.

The study of various geometric characteristics along evolution of density operators is becoming increasingly important and deserves special care [37]. For this reason, we leave the quantitative analysis of the physical usefulness of the efficiency measures η and $\tilde{\eta}$ in Eq. (A1) (and Eq. (A2)) and Eq. (A3) in analog quantum searching and precision metrology to forthcoming efforts.

Appendix B: Small energy difference regime

In this Appendix, we comment for the sake of mathematical completeness on the geodesic constraint equation $d^2(t, \lambda) = 0$ in the case of the small energy difference regime, although our main focus in the manuscript is devoted to the large energy difference regime specified by $E' \gg E$.

When we relax the working condition $E' \gg E$ and consider the low energy difference scenario where $E' \stackrel{\text{def}}{=} \gamma E$ and E are sufficiently close with $E' > E$, imposing $d^2(t, \lambda)$ in Eq. (35) to be equal to zero requires that the quantum overlap x satisfies the condition $x^2 = x^2(n, \gamma)$ where,

$$x^2(n, \gamma) \stackrel{\text{def}}{=} \frac{1}{64\gamma n^2} [(1 - 16n^2)\gamma^2 + (2 + 32n^2)\gamma + (1 - 16n^2)], \quad (\text{B1})$$

with $n \in \mathbb{N}$ and $\gamma > 1$. A simple calculation shows that x^2 in Eq. (B1) assumes positive values on the set $\mathcal{I}_n \stackrel{\text{def}}{=} [i_-(n), i_+(n)]$ with $i_{\pm}(n) \stackrel{\text{def}}{=} (32n^2 \pm 16n + 2)/(32n^2 - 2)$. However, \mathcal{I}_n is a set whose measure vanishes asymptotically since $\mu(\mathcal{I}_n) \stackrel{\text{def}}{=} 16n/(16n^2 - 2) \stackrel{n \gg 1}{\approx} 1/n \rightarrow 0$ when n approaches infinity. In summary, the set \mathcal{I}_n tend to shrink and eventually, vanish. Moreover, the set \mathcal{I}_n contains elements that violate the condition $\gamma > 1$. Indeed, $i_-(n) > 1$ if and only if $n < 1/4$. Clearly, this is impossible since $n \in \mathbb{N}$. In particular, for any $\gamma > i_+(1) \stackrel{\text{def}}{=} 5/3$ with $5/3$ being the upper bound of the set \mathcal{I}_n with the largest measure, that is \mathcal{I}_1 with $\mu(\mathcal{I}_1) = 16/15$, x^2 in Eq. (B1) becomes negative. Thus, we can conclude that Eq. (36) has no solution x that belongs to the interval $(0, 1)$ for any real $\gamma > i_+(1)$. Interestingly, the limit of large n values can also be physically motivated. Indeed, from a physics standpoint, we expect t_{MFG} to become very large when $E' \gtrsim E$ in the study of the quantum mechanical evolution between nearly orthogonal quantum states with nearly zero quantum overlap since t_{MFG} is inversely proportional to the energy level separation of the system and this equals $[4x^2\gamma + (1 - \gamma)^2] E$ [31, 46]. Imposing the condition expressed in Eq. (36), the long time limit is recovered when $n \gg 1$ since such a condition requires t_{MFG} to be proportional to n with constant of proportionality coefficient given by $2h/(E' + E)$. As a side remark, this long time limit is reminiscent of the infinite temporal duration of highly efficient ideal reversible thermodynamic processes that occur in the absence of dissipation. In summary, we can safely conclude from our discussion that $x \notin (0, 1)$ for any positive integer $\gamma \in \mathbb{Z}_+$ with $\gamma > 1$ in any of the two energetic regimes (that is, $E' \gg E$ and $E' > E$) of the modified quantum search scenario if $d^2(t, \lambda)$ in Eq. (35) is required to be identically zero.